Bisanthracene Bis(dicarboxylic imide)s as Potential Photosensitizers in Photodynamic Therapy: A Theoretical Investigation

Marta E. Alberto,[†] Cristina Iuga,[‡] Angelo D. Quartarolo,[†] and Nino Russo[†,§,*]

[†]Dipartimento di Chimica e Tecnologie Chimiche, Università della Calabria, 87036 Rende, Italy

[‡]Universidad Autónoma Metropolitana-Azcapotzalco, Departamento de Ciencias Básicas Av. San Pablo 180, México D.F. 02200, México

[§]Departamento de Quimica, Division de Ciencias Basicas e Ingenieria, Universidad Autonoma Metropolitana-Iztapalapa, Av. San Rafael Atlixco No.186, Col. Vicentina, CP 09340, Mexico, D.F., Mexico

Ⓢ *Supporting Information*

ABSTRACT: The electronic structures and spectroscopic properties of four bisanthracene bis-(dicarboxylic imide)s (M1−M4) have been investigated theoretically by using density functional theory (DFT) and its time-dependent extension (TDDFT) in view of their potential use as photosensitizers in photodynamic therapy (PDT). The optimized geometries, electronic absorption transitions, singlet−triplet energy gaps, spin−orbit matrix elements, ionization potentials, and electron affinities have been determined in gas phase and in solvent. Both type I and II PDT mechanisms have been considered. In addition, the variation of a series of relevant properties upon heavy atom substitution (Br and I) have been determined and discussed. Results show that only M4 is able to support the type I reaction, and one of its brominated and iodinated derivatives can produce cytotoxic singlet oxygen (type II reaction).
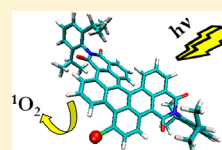
■ INTRODUCTION

Polycyclic aromatic hydrocarbons (PAHs), such as rylenes and their dicarboxylic imide derivatives, have been proposed as near-infrared (NIR) dyes due to their solubility, photophysical stability, and absorption and/or emission properties.[1,2] Their potential technological applications range from dye-sensitized solar cells, optical storage devices, and fluorescent probes.
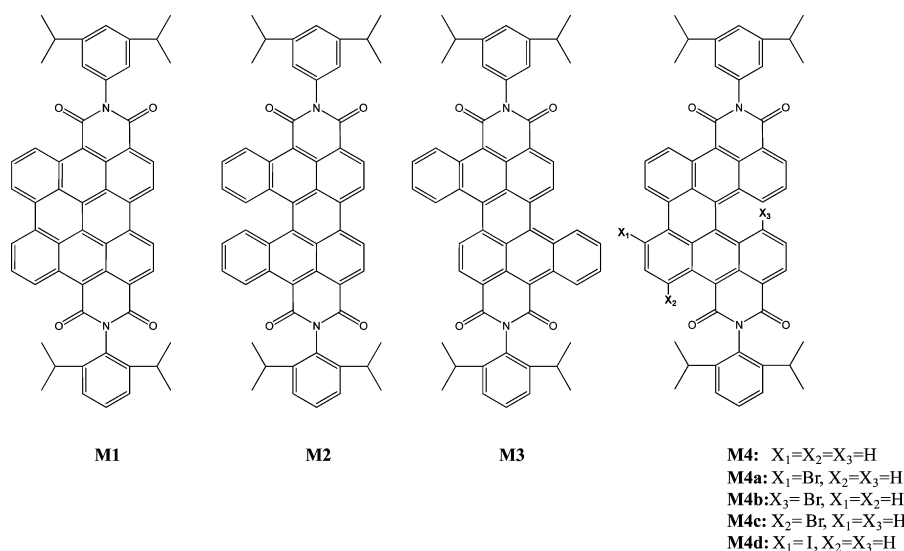
Recently, a series of soluble and stable dibenzoperylene derivatives and laterally expanded bisanthracene bis-(dicarboxylic imide)s have been synthesized and characterized, and their photophysical and electrochemical properties have been studied.[3] These systems (Scheme 1) show an absorption band in the NIR region and a great photostability. In principle, these molecules can be proposed also for their use in photodynamic therapy (PDT) because they show an absorption Q-band that falls in the so-called therapeutic window (from 500 to 850 nm). Furthermore, in the recent past, similar molecules such a series of perylenediimide systems have been tested in vitro as singlet oxygen generators in the light-assisted treatment of tumor diseases.[4−6] For these reasons, we have undertaken a theoretical study in order to determine the crucial photophysical properties (electronic transitions, singlet−triplet energy gap, vertical ionization, and electron affinities and spin−orbit coupling constants) essential to characterize these systems as effective drugs in PDT.

PDT is a non-invasive medical technique for the treatment of different types of diseases in oncology (e.g., like skin, breast, prostate, and bladder cancer), ophthalmology (age-related macular degeneration), dermatology (psoriasis), arteriosclerosis, and genecology.[7−11] In addition, PDT can be used in environmental application to catalyze pollutant degradation and water disinfection.[12,13] In PDT, a photosensitizer (Ps) is excited by an appropriate light source from its ground state S_0 to the first excited one S_1 and then through a radiationless intersystem crossing transition (ISC) to generate the triplet (T_1) electronic state. The activated sensitizer can undergo two kinds of reactions: (i) It can react directly, either with the substrate such as the cell membrane or a molecule, transfer an electron or hydrogen atom to yield radical ions and free radicals. These radicals are subsequently scavenged by oxygen to produce oxygenated products (type I reaction). (ii) The T_1 excited sensitizer can transfer its energy to the ground state of molecular oxygen ($^3\Sigma_g^-$ or $^3O_2$) to yield the cytotoxic excited singlet oxygen agent ($^1\Delta_g$ or $^1O_2$), which reacts with many biological molecules, including lipids, proteins, and nucleic acids, leading to cancer cell death. From a photophysical point of view, a clinically successful Ps agent able to generate a type II photochemical reaction must have a singlet−triplet energy gap of about 0.98 eV, which is crucial for $^1O_2$ generation, corresponding to the $^3\Sigma_g^- \rightarrow {}^1\Delta_g$ electronic transition for molecular oxygen.[14] In order to increase the singlet oxygen quantum yield, Φ_Δ, heavy atoms such as halogens (Br, I) or transition metal atoms can be introduced in the molecular structure. The presence of an atom with a high atomic number causes the mixing of pure electronic states of different spin multiplicity (the so-called heavy atom or spin−orbit coupling effect), thus increasing the rate of the intersystem spin crossing between S_1 and T_1 states ($S_1 \rightarrow T_1$ radiationless transition).[15,16] When the triplet lifetime is sufficiently long-lived (typically on the order of few μs), the energy transfer from the T_1 photosensitizer state to $^3O_2$ is favored and consequently Φ_Δ

Scheme 1. Chemical Structures of Bisanthene bis(dicarboxylic imide) (M1) and Partially Cyclized Bisanthene(dicarboxylic amide)s (M2−M4)

M1   M2   M3

M4: $X_1 = X_2 = X_3 = H$
M4a: $X_1 = Br$, $X_2 = X_3 = H$
M4b: $X_3 = Br$, $X_1 = X_2 = H$
M4c: $X_2 = Br$, $X_1 = X_3 = H$
M4d: $X_1 = I$, $X_2 = X_3 = H$

Table 1. Main Vertical Singlet Electronic Energies ΔE, Oscillator Strengths, f, and Main Configuration for Compounds M1−M4 in Water and Dichloromethane Solvents

	PBE0/6-31G*			ωB97XD/6-31G*			
molecule	ΔE (eV, nm)	configuration	f	ΔE (eV, nm)	configuration	f	exptl.
			water				
M1	1.478, 839	H → L, 71%	0.423	1.668, 743	H → L, 70.1%	0.112	
M2	1.788, 694	H → L, 71%	0.558	2.007, 618	H → L, 69.8%	0.853	
M3	1.798, 689	H → L, 71.1%	0.583	2.019, 614	H → L, 69.8%	0.882	
M4	1.802, 688	H → L, 70.9%	0.484	2.054, 604	H → L, 69.7%	0.747	
M4a	1.766, 702	H→ L, 70.8%	0.568				
M4b	1.676, 740	H→ L, 70.8%	0.573				
M4c	1.652, 751	H→ L, 70.8%	0.520				
M4d	1.745, 710	H→ L, 70.7%	0.542				
			dichloromethane				
M1	1.405, 882	H → L, 71%	0.553	1.686, 735	H → L, 70.1%	0.789	830
M2	1.711, 724	H → L, 70.9%	0.687	2.021, 613	H → L, 69.8%	0.856	697
M3	1.710, 725	H → L, 71%	0.710	2.035, 609	H → L, 69.8%	0.890	697
M4	1.742, 712	H → L, 70.8%	0.601	2.084, 595	H → L, 69.7%	0.760	685

increases. Different classes of compounds have been proposed or currently approved as photosensitizers in PDT. Mainly, they are porphyrin-like class of molecules[17,18] such as photophrin, a mixture of hematoporphyrin monomers, dimers, and oligomers[19] (first accepted PDT drugs for the treatment of early stage lung cancer), m-tetrahydroxyphenylchlorin (mTHPC, Foscan),[20] and lutetium texaphyrin (Lutrin)[21,22] that are in the advanced phase of clinical tests or already accepted for clinical use. Recently, new non-porphyrin systems (e.g., phenotiazinium, tetra-aryl-azadipyrromethenes, squaraines, or hypericin derivatives) have been synthesized, characterized, and proposed as potential PDT drugs.[23−27]

In this work, we present a detailed theoretical investigation of the photophysical properties of four recently synthesized bisanthracene bis(dicarboxylic imide) systems (Scheme 1) in order to verify if they can be proposed as photosensitizers in PDT following the type I or type II mechanism. By means of the TDDFT approach, we have investigated the electronic absorption spectra, providing singlet−triplet energy gaps, vertical ionization potentials, and electron affinities, together with data concerning the magnitude of the spin−orbit coupling.

Furthermore, in order to evaluate the heavy atom effect on the photophysical properties of such systems, we have considered also some halogenated derivatives of one of the tested molecules (Scheme 1) introducing a bromine and an iodine in different positions of the molecular skeleton.

■ **COMPUTATIONAL DETAILS**

All the computations presented in this work have been carried out by using Gaussian 09[28] code at DFT and its time-dependent formulation TDDFT[29] levels of theory. Full structures optimization have been performed in solvent by means of the SMD continuum solvent model[30] setting up the dielectric constants of water and dichloromethane along with the default cavity generation parameters. The hybrid PBE0[31,32] and the long-range corrected hybrid ωB97XD[33,34] exchange−correlation functional have been employed combined with the 6-31G* basis set for all atoms[35] except for iodine, which was described by the quasi-relativistic Stuttgart−Dresden pseudo-potentials.[36] The vibrational analysis has been carried out at the same level of theory giving all real eigenvalues for the Hessian

matrix. The TDDFT[29] calculations have been carried out on the ground state equilibrium structures using the same basis set as for the optimizations and testing both the PBE0 and ωB97XD functionals, previously successfully used to reproduce the absorption spectra of different molecules, including photosensitizers active in PDT.[37−49] The vertical triplet energies have been obtained over the ground state (S_0) electronic configuration in solvent. The same procedures have been used in order to obtain the vertical ionization potentials[45] and electron affinities of the lowest-lying singlet (VIP, VEA) and triplet states (VIP(T_1), VEA(T_1)). Spin−orbit matrix elements have been computed by using the DALTON code[50] employing both the Breit−Pauli method[51] and atomic-mean field approximation.[52] Because in DALTON a few hybrid functionals are available to perform these calculations, B3LYP[53,54] has been used on the previously PBE0-optimized geometries.

■ RESULTS AND DISCUSSION

Geometrical Structures. The optimized structure of the bisanthracene bis(dicarboxylic imide) molecules results to be planar in the aromatic cores, while the phenyl rings linked on the nitrogen atoms are tilted out of the central aromatic plane. This is also due to the presence of two −C(CH$_3$)$_3$ groups in the para position that causes a considerable steric hindrance. In dichloromethane solvent, the torsional angles are found to be 89.4 (89.3), 89.8 (88.0), 86.9 (86.6), and 86.9 (87.0) degrees for N1, M2, M3, M4, respectively, at PBE0 and (ωB97XD) levels of theory. Similar values have been determined performing the optimizations in water solvent.

Electronic Absorption Spectra. The obtained photophysical properties together with the available experimental results are reported in Table 1. All the considered systems show a strong Q-band. In dichloromethane solvent, PBE0 exchange−correlation functional predicts excitation energies of 830, 697, 697, and 685 nm for M1, M2, M3, and M4, respectively. The agreement with the experimental data obtained in dichloromethane is very satisfactory (the maximum deviation is 62 nm and concerns the M1 molecule), and the simulated transitions are all shifted in the red region. Looking at Table 1, it is evident that in the water solvent all the excitation energies are blue shifted by 41 nm in the case of M1 and about 24 nm for the other systems. The use of the long-range corrected ωB97XD functional reveals a systematic blue shift for both the considered solvents of about 100 nm with respect to the PBE0 and experimental counterparts. For all the compounds, we find that the transition is mainly HOMO−LUMO (H-L) in nature (about 71%) with some small contribution coming from other excitations (Table 1). The HOMO (H) and LUMO (L) orbitals pictures are delocalized over all the structures (Supporting Information), so we can conclude that Q-band is essentially due to a $\pi-\pi^*$ transition. The compound that shows the absorption band at the highest wavelength, falling in the NIR region, is M1. As can be deduced from Figure 1, such a transition is directly related to the smaller H-L gap calculated for the M1 molecule. On the contrary, in the case of the M4 compound, the wavelength of the light absorbed is lower due to the larger obtained energy gap.

The increase in H-L gap going from M1 to M4 is essentially due to a slighter stabilization of the H in M2−M4 and a smaller destabilization of the L energies for the same compounds. The combined effects of these two behaviors render M4 the molecule with higher H-L gap.
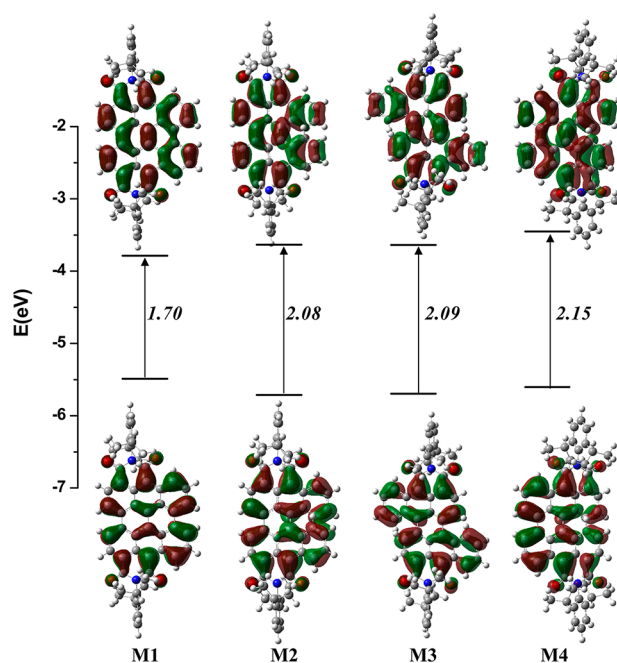
Figure 1. Partial energetic diagram (eV) for the highest occupied and lowest virtual unoccupied molecular orbitals of molecules M1−M4. The HOMO−LUMO energy gaps, indicated by solid arrows, and their molecular pictures are shown.

Nevertheless, it is noteworthy that all the investigated compounds have an absorption band that falls in the PDT therapeutic window. The presence of the heavy atom does not affect significantly the Q absorption band. In fact, we obtain in a water solvent and by using the PBE0 exchange−correlation functional absorption bands located at 702, 740, and 751 nm for the bromine in the three different positions (M4a, M4b, and M4c). The presence of iodine shifts the absorption band at 710 nm (Table 1).

Type II Reaction. As previously mentioned, the S_1 energy can be transferred to the T_1 state through an intersystem crossing. If the T_1 energy of the photosensitizer lies above the energy necessary to activate the ground state molecular oxygen (0.98 eV) ($^3O_2$), the singlet oxygen ($^1O_2$) species can be generated

$$Ps(T_1) + {}^3O_2 \rightarrow Ps(S_0) + {}^1O_2$$
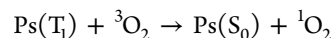
In order to verify if this process occurs, first of all we must compute the photosensitizer singlet−triplet energy gaps (ΔE_{S-T}). Results are reported in Table 2. From this table, it is clear that all the compounds show ΔE_{S-T} sensibly lower to

Table 2. Vertical Singlet−Triplet Energy Gap in eV (ΔE_{S-T}) Computed in Water at PBE0/6-31G* Level of Theory

| molecule	ΔE_{S-T}
M1	0.52
M2	0.88
M3	0.87
M4	0.94
M4a	1.02
M4b	0.89
M4c	0.88
M4d	1.02

the 0.98 eV necessary to activate the singlet oxygen. The lowest value is with M1 (0.52 eV), while the highest is obtained with M4 (0.94 eV). Because the presence of a heavy atom can increase the singlet–triplet energy gap, we have considered of interest to add a bromine atom in different positions of M4 (Scheme 1), showing this compound with a ΔE_{S-T} close to 0.98 eV. In the M4a brominated derivative, we found an increased gap equal to 1.02 eV. Furthermore, to see the effect of the dimension of the substituted heavy atom, we have considered in the same position an iodine atom. In this case, the ΔE_{S-T} reaches the value of 1.04 eV. On the basis of these results, both bromine and iodine derivatives are, in principle, able to activate the singlet oxygen. The singlet oxygen production will depend also on the efficiency of the intersystem crossing (radiationless transition $S_1 \rightarrow T_1$ rate constants) that in turn depends on the amplitude of the spin–orbit coupling. This last term is proportional to the squared module of the spin–orbit Hamiltonian matrix element between the initial Ψ (S_1) and final Ψ (T_1) wave functions. Moreover, it can depend on the nature of the orbitals involved in the transition, and in general, it can be increased by the presence of a heavy atom. For this reason, we have computed the spin–orbit matrix elements for M4 as well as for their brominated and iodinated derivatives (Table 3). For M1–M4 and M4a, both the Breit–Pauli

method[51] and the atomic-mean field approximation[52] have been used. As shown in Table 3, the obtained results are very similar, and because the Breit-Pauli method is very time expensive, for the other systems, only the second approach has been employed. Comparing the values for all the compounds, we note that the introduction of a heavy atom significantly increases the spin–orbit coupling, and it appears to be related to the atomic number of the substituted atom. In fact, the presence of iodine in the M4d derivative gives a spin–orbit matrix elements higher than the corresponding bromine atom in the same position.

On the basis of our results, it emerges that although none of the compounds M1–M4 are able to a generate singlet oxygen species, the bromine- or iodine-functionalized M4 compound (M4a and M4d) possesses all the chemical and physical properties able to indicate these compounds as possible candidates to generate a type II reaction in PDT.

Type I Reactions. As shown in the previous section, compounds M1–M4 are unable to generate cytotoxic singlet oxygen, nevertheless they could be active in PDT through the generation of a type I reaction. In these kinds of reactions, different mechanisms are possible. In the main channel, it is supposed that the excited triplet state of the photosensitizer ($^3Ps^*$) oxidizes the substrate (S) through the reaction

$$^3Ps^* + S - > Ps^{\cdot(-)} + S^{\cdot(+)} \qquad (a)$$
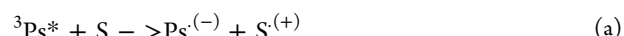
and then the reduced photosensitizer reacts with molecular dioxygen producing the superoxide radical ion

$$Ps^{\cdot(-)} + {}^3O_2 \rightarrow {}^1Ps + O_2^{\bullet(-)} \qquad (b)$$
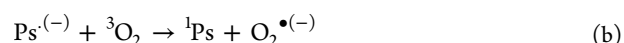
The superoxide anion can generate other highly reactive radicals (e.g., hydroxyl) that promote reactions with biomolecules.

The crucial step of this mechanism, supposing that the $^3Ps^*$ oxidizes the biological substrate (e.g., DNA nucleic acid base, or amino acids, or lipids), is the generation of the superoxide ion. Following the reaction b, this is possible only if VEA($^3O_2$) – VEA Ps (S_0/T_1) > 0.

Another possibility to produce $O_2^{\bullet(-)}$ is the photo-oxidation of the photosensitizer in the ground (S_0) or excited states (T_1), according to the following reaction

$$Ps(S_0/T_1) + {}^3O_2 \rightarrow Ps^{\bullet(+)} + O_2^{\bullet(-)} \qquad (c)$$
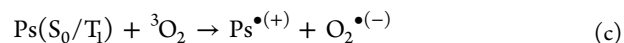
Table 3. Spin–Orbit Cartesian Matrix Elements (values in cm^{-1}) between First Lowest Singlet and Triplet Excited States, Calculated at the B3LYP/6-31G(d)//PBE0

molecule	$\hat{H}_{so}^x$	$\hat{H}_{so}^y$	$\hat{H}_{so}^z$
M2	0.24^a	0.0	0.12^a
	(0.23)^b	(0.0)^b	(0.12)^b
M3	−0.06^a	0.0^a	0.0^a
	(−0.03)^b	0.0^b	0.0^b
M4	0.04^a	0.0^a	0.02^a
	(−0.01)^b	(0.0)^b	(0.0)^b
M4a	−2.22	0.24	0.09
	(−2.21)^b	(0.25)^b	(0.04)^b
M4b	(4.55)^b	(0.69)^b	(1.48)^b
M4c	(−1.10)^b	(0.73)^b	(1.93)^b
M4d	(−12.9)^b	(1.49)^b	(−1.55)^b

^{a}Breit–Pauli method. ^{b}Atomic-mean field approximation.

Table 4. Vertical Electron Affinities (VEA) and Ionization Potentials (VIP), for M1–M4 compounds Together with Corresponding Values for the First Triplet Excited State VEA(T$_1$) and VIP(T$_1$) in Water and Dichloromethane Solvents

molecule	PBE0/6-31G*				ωB97XD/6-31G*			
	VEA(T$_1$) (eV)	VEA (eV)	VIP(T$_1$) (eV)	VIP (eV)	VEA(T$_1$) (eV)	VEA (eV)	VIP(T$_1$) (eV)	VIP (eV)
				water				
M1	−4.49	−4.09	4.82	5.14	−4.36	−3.98	4.91	5.16
M2	−4.61	−3.95	4.77	5.36	−4.47	−3.81	4.88	5.45
M3	−4.65	−3.95	4.74	5.35	−4.55	−3.81	4.83	5.45
M4	−4.49	−3.77	4.61	5.25	−4.36	−3.62	4.71	5.33
				dichloromethane				
M1	−4.23	−3.83	4.91	5.22	−4.12	−3.73	5.00	5.27
M2	−4.34	−3.69	4.85	5.44	−4.20	−3.54	4.95	5.53
M3	−4.39	−3.69	4.82	5.42	−4.28	−3.54	4.91	5.53
M4	−4.24	−3.51	4.70	5.35	−4.11	−3.36	4.80	5.45

In this case, the reaction occurs via direct electron transfer from Ps to oxygen or in other terms if the following condition is satisfied

$$VEA(^3O_2) > VIP(Ps(S_0/T_1))$$

Finally, we have considered also some autoionization processes

$$Ps(T_1) + Ps(S_0) - > Ps^{\bullet(+)} + Ps^{\bullet(-)} \qquad (d)$$

$$Ps(T_1) + Ps(T_1) - > Ps^{\bullet(+)} + Ps^{\bullet(-)} \qquad (e)$$
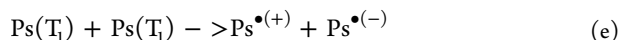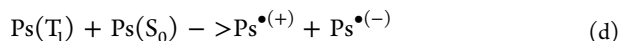
In these last cases, from a thermodynamic point of view, the auto-ionization occurs if for each photosensitizer

$$VEA(T_1) > VIP(S_0)$$

$$VEA(T_1) > VIP(T_1)$$

In order to verify these possibilities, we have computed the PBE0 and ωB97XD vertical electron affinities and ionization potential for both the singlet and triplet electronic states of compounds M1−M4. Results are collected in Table 4. Considering that the computed $VEA(^3O_2)$ at PBE0 in water is 3.87 eV,[45] the following considerations can be drawn: (i) Reaction b is thermodynamically exothermic only for compound M4 in its ground state (S_0) and in both the considered solvents. (ii) Reactions c, d, and e do not occur for all the considered compounds.

On the basis of these considerations, only compound M4 could be active in type I PDT reactions with a mechanism in which an electron transfer from the reduced photosensitizer to ground state molecular oxygen (reaction b) occurs.

CONCLUSIONS

Four bisanthracene bis(dicarboxylic imide)s systems have been the subject of a detailed DFT and TDDFT investigation with the aim to rationalize their electronic and spectroscopic structures and to verify if these molecules can be proposed as potential PDT photosensitizers. Results show the following: (1) All the compounds show electronic transition energies that fall in the so-called therapeutic window. (2) The computed singlet−triplet energy gaps for the unsubstituted systems result in lower energy than that required to generate a cytotoxic single oxygen via type II reaction. (3) The introduction of a bromine or iodine heavy atom to give M4a and M4d compounds increases the ΔE_{S-T} gap as well as the spin orbit matrix elements. These two substituted compounds can be proposed as PDT singlet oxygen producers. (4) M4 system could be active in PDT throughout a type I reaction mechanism. In particular, it is able to transfer an electron to the ground state molecular oxygen generating the superoxide.

ASSOCIATED CONTENT

Ⓢ Supporting Information

Frontier molecular orbitals for compounds M1−M4 in water solvent are reported in Figure S1. This material is available free of charge via the Internet at http://pubs.acs.org.

AUTHOR INFORMATION

Corresponding Author

*E-mailnrusso@unical.it.

Author Contributions

The manuscript was written through contributions of all authors. All authors have given approval to the final version of the manuscript.

Notes

The authors declare no competing financial interest.

REFERENCES

(1) Herrmann, A.; Mullen, K. From industrial colorants to single photon sources and biolabels: The fascination and function of rylene dyes. *Chem. Lett.* **2006**, *35*, 978−985.

(2) Pschirer, N. G.; Kohl, C.; Nolde, F.; Qu, J.; Müllen, K. Pentarylene- and Hexarylenebis(dicarboximide)s: Near-infrared-absorbing polyaromatic Dyes. *Angew. Chem.* **2006**, *118*, 1429−1432; *Angew. Chem., Int. Ed.* **2006**, *45*, 1401−1404.

(3) Yao, J. H.; Chi, C.; Wu, J.; Loh, K.-P. Bisanthracene bis(dicarboxylic imide)s as soluble and stable NIR dyes. *Chem.— Eur. J.* **2009**, *15*, 9299−9302.

(4) MacDonald, I. J.; Dougherty, T. J. Basic principles of photodynamic therapy. *J. Porphyrins Phthalocyanines* **2001**, *5*, 105−129.

(5) Dolmans, D. E.; Fukumura, D.; Jain, R. K. Photodynamic therapy for cancer. *Nat. Rev. Cancer* **2003**, *3*, 380−387.

(6) Allison, R. D.; Downie, G. H.; Cuenca, R.; Hu, X.; Childs, C. J. H.; Sibata, C. H. Photosensitizers in clinical PDT. *Photodiagn. Photodyn. Ther.* **2004**, *1*, 27−42.

(7) Stockert, J. C.; Cañete, M.; Juarranz, A.; Villanueva, A.; Horobin, R. W.; Borrell, J. I.; Teixidó, J.; Nonell, S. Porphycenes: Facts and prospects in photodynamic therapy of cancer. *Curr. Med. Chem.* **2007**, *14*, 997−1026.

(8) Dougherty, T. J.; Gomer, C. J.; Henderson, B. W.; Jori, G.; Kessel, D.; Korbelik, M.; Moan, J.; Peng, Q. Photodynamic therapy. *J. Natl. Cancer Inst.* **1998**, *90*, 889−905.

(9) Bonnett, R. In *Chemical Aspects of Photodynamic Therapy*; Gordon & Breach Science Publishers: Amsterdam, 2000; pp 1−289.

(10) Juzeniene, A.; Peng, Q.; Moan, J. Milestones in the development of photodynamic therapy and fluorescence diagnosis. *J. Photochem. Photobiol. Sci.* **2007**, *6*, 1234−1245.

(11) Schuitmaker, J. J.; Baas, P.; van Leengoed, H. L. L. M.; van der Meulen, F. W.; Star, W. M.; van Zandwijk, N. Photodynamic therapy: a promising new modality for the treatment of cancer. *J. Photochem. Photobiol, B* **1996**, *34*, 3−12.

(12) Chong, M. N.; Jin, B.; Chow, C. W. K.; Saint, C. Recent developments in photocatalytic water treatment technology: A review. *Water Res.* **2010**, *44*, 2997−3027.

(13) Sunnotel, O.; Verdoold, R.; Dunlop, P. S. M.; Snelling, W. J.; Lowery, C. J.; Dooley, J. S. G.; Moore, J. E.; Byrne, J. A. Photocatalytic inactivation of *Cryptosporidium parvum* on nanostructured titanium dioxide films. *J. Water Health* **2010**, *8*, 83−91.

(14) Herzberg, G. In *Spectra of Diatomic Molecules*, 2nd ed.; Van Nostrand Reinhold: New York, 1950; pp 344−346.

(15) Darmanyan, A. P.; Foote, C. S. Effect of sensitizer heavy atoms on singlet oxygen generation efficiency. *J. Phys. Chem.* **1992**, *96*, 3723−3728.

(16) Turro, N. J. In *Modern Molecular Photochemistry*; Benjamin: Menlo Park, 1978; pp 153−198.

(17) Nyman, E. S.; Hynninen, P. H. Research advances in the use of tetrapyrrolic photosensitizers for photodynamic therapy. *J. Photochem. Photobiol., B* **2004**, *73*, 1−28.

(18) Sternberg, E. D.; Dolphin, D.; Bruckner, C. Porphyrin-based photosensitizers for use in photodynamic therapy. *Tetrahedron* **1998**, *54*, 4151–4202.

(19) Lipson, R. L.; Baldes, E. J. The photodynamic properties of a particular hematoporphyrin derivative. *Arch. Dermatol.* **1960**, *82*, 508–516.

(20) Ronn, A. M.; Nouri, M.; Lofgren, L. A.; Steinberg, B. M.; Westerborn, A.; Windahl, T.; Shikowitz, M. J.; Abramson, A. L. Human tissue levels and plasma pharmacokinetics of temoporfin (Foscan, mTHPC). *Lasers Med. Sci.* **1996**, *11*, 267–272.

(21) Young, S. W.; Woodburn, K. W.; Wright, M.; Mody, T. D.; Fan, Q.; Sessler, J. L.; Dow, C.; Miller, R. A. Lutetium texaphyrin (PCI-0123): A near-infrared, water-soluble photosensitizer. *Photochem. Photobiol.* **1996**, *63*, 892–897.

(22) Hsi, R. A.; Kapatkin, A.; Strandberg, J.; Zhu, T.; Vulcan, T.; Solonenko, M.; Rodriguez, C.; Chang, J.; Saunders, M.; Mason, N.; Hahn, S. Photodynamic therapy in the canine prostate using motexafin lutetium. *Clin. Cancer Res.* **2001**, *7*, 651–660.

(23) O'Connor, A. E.; William, M.; Gallagher, W. M.; Byrne, A. T. Porphyrin and nonporphyrin photosensitizers in oncology: Preclinical and clinical advances in photodynamic therapy. *Photochem. Photobiol.* **2009**, *85*, 1053–1074.

(24) Wainwright, M. Non-porphyrin photosensitizers in biomedicine. *Chem. Soc. ReV.* **1996**, *25*, 351–359.

(25) New, O. M.; Dolphin, D. Design and synthesis of novel phenothiazinium photosensitiser derivatives. *Eur. J. Org. Chem.* **2009**, *16*, 2675–2686.

(26) Gorman, A.; Killoran, J.; O'Shea, C.; Kenna, T.; Gallagher, W. M.; O'Shea, D. F. In Vitro Demonstration of the heavy-atom effect for photodynamic therapy. *J. Am. Chem. Soc.* **2004**, *126*, 10619–10631.

(27) Ramaiah, D.; Eckert, I.; Arun, K. T.; Weidenfeller, L.; Epe, B. Squaraine dyes for photodynamic therapy: study of their cytotoxicity and genotoxicity in bacteria and mammalian cells. *Photochem. Photobiol.* **2002**, *76*, 672–677.

(28) Gaussian 09, Revision A.2, Frisch, M. J.; Trucks, G. W.; Schlegel, H. B.; Scuseria, G. E.; Robb, M. A.; Cheeseman, J. R.; Scalmani, G.; Barone, V.; Mennucci, B.; Petersson, G. A.; Nakatsuji, H.; Caricato, M.; Li, X.; Hratchian, H. P.; Izmaylov, A. F.; Bloino, J.; Zheng, G.; Sonnenberg, J. L.; Hada, M.; Ehara, M.; Toyota, K.; Fukuda, R.; Hasegawa, J.; Ishida, M.; Nakajima, T.; Honda, Y.; Kitao, O.; Nakai, H.; Vreven, T.; Montgomery, Jr., J. A.; Peralta, J. E.; Ogliaro, F.; Bearpark, M.; Heyd, J. J.; Brothers, E.; Kudin, K. N.; Staroverov, V. N.; Kobayashi, R.; Normand, J.; Raghavachari, K.; Rendell, A.; Burant, J. C.; Iyengar, S. S.; Tomasi, J.; Cossi, M.; Rega, N.; Millam, J. M.; Klene, M.; Knox, J. E.; Cross, J. B.; Bakken, V.; Adamo, C.; Jaramillo, J.; Gomperts, R.; Stratmann, R. E.; Yazyev, O.; Austin, A. J.; Cammi, R.; Pomelli, C.; Ochterski, J. W.; Martin, R. L.; Morokuma, K.; Zakrzewski, V. G.; Voth, G. A.; Salvador, P.; Dannenberg, J. J.; Dapprich, S.; Daniels, A. D.; Farkas, Ö.; Foresman, J. B.; Ortiz, J. V.; Cioslowski, J.; Fox, D. J. Gaussian, Inc., Wallingford CT, 2009.

(29) Casida, M. E. In *Recent Developments and Applications in Density-Functional Theory*; Seminario, J. M., Ed.; Elsevier: Amsterdam, The Netherlands, 1996; pp 155–192.

(30) Marenich, A. V.; Cramer, J.; Truhlar, D. G. Universal solvation model based on solute electron density and on a continuum model of the solvent defined by the bulk dielectric constant and atomic surface tensions. *J. Phys. Chem. B* **2009**, *113*, 6378–6396.

(31) Adamo, C.; Barone, V. Toward reliable density functional methods without adjustable parameters: The PBE0 model. *J. Chem. Phys.* **1999**, *110*, 6158–6170.

(32) Ernzerhof, M.; Scuseria, G. E. Assessment of the Perdew–Burke–Ernzerhof exchange–correlation functional. *J. Chem. Phys.* **1999**, *110*, 5029–5036.

(33) Chai, J. D.; Head-Gordon, M. J. Systematic optimization of long-range corrected hybrid density functional. *Chem. Phys.* **2008**, *128*, 84106–84155.

(34) Chai, J. D.; Head-Gordon, M. Long-range corrected hybrid density functionals with damped atom–atom dispersion corrections. *Phys. Chem. Chem. Phys.* **2008**, *10*, 6615–6620.

(35) (a) Ditchfield, R.; Hehre, W. J.; Pople, J. A. Self-consistent molecular-orbital methods. IX. An extended Gaussian-type basis for molecular-orbital studies of organic molecules. *J. Chem. Phys.* **1971**, *54*, 724–728. (b) Hehre, W. J.; Ditchfield, R.; Pople, J. A. Self-consistent molecular orbital methods. XII. Further extensions of Gaussian—Type basis sets for use in molecular orbital studies of organic molecules. *J. Chem. Phys.* **1972**, *56*, 2257–2261.

(36) Andrae, D.; Haussermann, U.; Dolg, M.; Stoll, H.; Preuss, H. Energy-adjusted ab initio pseudopotentials for the second and third row transition elements. *Theor. Chim. Acta* **1990**, *77*, 123–141.

(37) Jacquemin, D.; Perpete, E. A.; Ciofini, I.; Adamo, C. Accurate simulation of optical properties in dyes. *Acc. Chem. Res.* **2009**, *42*, 326–334.

(38) Jacquemin, D.; Perpete, E. A.; Scuseria, G. E.; Ciofini, I.; Adamo, C. TD-DFT performance for the visible absorption spectra of organic dyes: Conventional versus long-range hybrids. *J. Chem. Theory Comput.* **2008**, *4*, 123–135.

(39) Eriksson, E. S. E.; Eriksson, L. A. Predictive power of long-range corrected functionals on the spectroscopic properties of tetrapyrrole derivatives for photodynamic therapy. *Phys. Chem. Chem. Phys.* **2011**, *13*, 7207–7217.

(40) Lanzo, I.; Russo, N.; Sicilia, E. First-principle time-dependent study of magnesium-containing porphyrin-like compounds potentially useful for their application in photodynamic therapy. *J. Phys. Chem. B* **2008**, *112*, 4123–4130.

(41) Quartarolo, A. D.; Russo, N.; Sicilia, E.; Lelj, F. Absorption spectra of the potential photodynamic therapy photosensitizers texaphyrins complexes: A theoretical analysis. *J. Chem. Theory Comput.* **2007**, *3*, 860–869.

(42) Quartarolo, A. D.; Russo, N.; Sicilia, E. Structures and electronic absorption spectra of a recently synthesised class of photodynamic therapy agents. *Chem.—Eur. J.* **2006**, *12*, 6797–6803.

(43) Quartarolo, A. D.; Sicilia, E.; Russo, N. On the potential use of squaraine derivatives as photosensitizers in photodynamic therapy: A TDDFT and RICC2 survey. *J. Chem. Theory Comput.* **2009**, *5*, 1849–1857.

(44) Quartarolo, A. D.; Lanzo, I.; Sicilia, E.; Russo, N. Can phthalocyanines and their substituted α-para-(methoxy)phenyl derivatives act as photosensitizers in photodynamic therapy? A TD-DFT study. *Phys. Chem. Chem. Phys.* **2009**, *11*, 4586–4592.

(45) Fortes Ramos Sousa, F.; Quartarolo, A. D.; Sicilia, E.; Russo, N. A time-dependent density functional study of a non-aromatic [1.1.1.1.1]-pentaphyrin and its lutetium complex. *J. Phys. Chem. B* **2012**, *116*, 10816–10823.

(46) Petit, L.; Adamo, C.; Russo, N. Absorption spectra of first-row transition metal complexes of bacteriochlorins: A theoretical analysis. *J. Phys. Chem. B* **2005**, *109*, 12214–12221.

(47) Petit, L.; Quartarolo, A.; Adamo, C.; Russo, N. Spectroscopic properties of porphyrin-like photosensitizers: Insights from theory. *Phys. Chem. B* **2006**, *110*, 2398–2404.

(48) Alberto, M. E.; De Simone, B. C.; Cospito, S.; Imbardelli, D.; Veltri, L.; Chidichimo, G.; Russo, N. Experimental and theoretical characterization of a new synthesized extended viologen. *Chem. Phys. Lett.* **2012**, *552*, 141–145.

(49) Bremond, E.; Alberto, M. E.; Russo, N.; Ricci, G.; Ciofini, I.; Adamo, C. Photophysical properties of NIR-emitting fluorescence probes: Insights from TD-DFT. *Phys. Chem. Chem. Phys.* **2013**, *15*, 10019–10027.

(50) DALTON, a molecular electronic structure program, Release Dalton 2011. http://daltonprogram.org/.

(51) Ågren, H.; Vahtras, O.; Knuts, S.; Jørgensen, P. Radiative lifetimes of triplet spin sublevels of the azabenzenes. *Chem. Phys.* **1994**, *181*, 291–304.

(52) Ruud, K.; Schimmelpfennig, B.; Ågren, H. Internal and external heavy-atom effects on phosphorescence radiative lifetimes calculated using a mean-field spin-orbit Hamiltonian. *Chem. Phys. Lett.* **1999**, *27*, 215–221.

(53) Becke, A. D. Density-functional exchange-energy approximation with correct asymptotic behavior. *Phys. Rev. A* **1988**, *38*, 3098–3100;

Density-functional thermochemistry 3. The role of exact exchange. *J. Chem. Phys.* **1993**, *98*, 5648−5652.

(54) Lee, C.; Yang, W.; Parr, R. G. Development of the Colle−Salvetti correlation−energy formula into a functional of the electron density. *Phys. Rev. B* **1988**, *37*, 785−789.

G

dx.doi.org/10.1021/ci4003365 | *J. Chem. Inf. Model.* XXXX, XXX, XXX−XXX